environmental sciences proceedings

MDPI

Proceeding Paper

Estimation of Surface Soil Moisture at the Intra-Plot Spatial Scale by Using Low and High Incidence Angles TerraSAR-X Images †

Rémy Fieuzal * and Frédéric Baup

[1] Centre d'Études de la BIOsphère (CESBIO), Université de Toulouse, CNES/CNRS/INRAe/IRD/UPS, 18 Avenue Edouard Belin, 31401 Toulouse, France; frederic.baup@cesbio.cnes.fr

* Correspondence: remy.fieuzal@cesbio.cnes.fr

† Presented at the 3rd International Electronic Conference on Geosciences, 7–13 December 2020; Available online: https://iecg2020.sciforum.net/#.

Abstract: The objective of this study is to analyze the capabilities of multi-temporal TerraSAR-X images to estimate the fine-scale SSM variability over bare agricultural plots (at a spatial scale ranging from 80 to 2800 m²). Time series of X-band satellite images were collected over a study site located in Southwestern France, together with intra-field measurements of key soil descriptors (i.e., SSM, surface roughness, and soil texture). The large dataset enables independent training and validating steps of a statistical algorithm (random forest), SSM being estimated using images acquired at low and high incidence angles. The levels of performance obtained at the plot spatial scale, with R^2 ranging from 0.64 to 0.67 (depending on the considered incidence angle) and an RMSE close to 5.0 $m^{-3}.m^{-3}$, are exceeded by those obtained at a finer scale (700 m², corresponding to buffers with a 15 m radius). At this intra-plot spatial scale, the estimates based on the low incidence angle images are associated with an R^2 of 0.69 and an RMSE of 4.89 $m^{-3}.m^{-3}$, results slightly lower than the performance obtained using high incidence angle images, R^2 of 0.72 and an RMSE of 4.55 $m^{-3}.m^{-3}$. Such magnitude of performance slightly increases over larger intra-plot spatial scales, the values of R^2 being superior to 0.75 with an RMSE lower than 4.20 $m^{-3}.m^{-3}$ over areas of 2800 m² (corresponding to buffers with a 30 m radius).

Keywords: surface soil moisture; bare soils; TerraSAR-X; random forest; plot spatial scale; intra-plot spatial scale

Citation: Fieuzal, R.; Baup, F. Estimation of Surface Soil Moisture at the Intra-Plot Spatial Scale by Using Low and High Incidence Angles TerraSAR-X Images. **2021**, *5*, 6. https://doi.org/10.3390/IECG2020-08528

Academic Editor: Jesus Martinez Frias

Published: 22 November 2020

1. Introduction

Numerous studies have demonstrated the usefulness of SAR satellite images for monitoring subsurface parameters, particularly in an agricultural context during periods without vegetation, where these signals offer the possibility of estimating variables related to the soil (e.g., surface soil moisture, surface roughness, and soil texture) [1–3]. The sensitivity of microwave signals to variations in surface soil moisture (SSM) has thus been demonstrated in various studies, and often quantified through empirical relationships [1,4,5]. In these studies, the dynamics of the signals are characterized, but the relationships remain nevertheless limited because they are established under specific conditions (on a limited number of plots or even on a single plot, for specific surface roughness levels, and/or on the basis of images acquired in specific configurations) limiting the possibilities of extrapolation over large areas.

To overcome these limitations of application in various contexts, other approaches have been proposed. For example, they are based on the following combination: electromagnetic signal modeling, in order to simulate the diversity of possible cases that can be observed in agricultural conditions, and a statistical inversion method, which is trained

on the basis of synthetic data from the modeling [6,7]. The target variable is finally estimated by applying the statistical algorithm to the satellite images. In this approach, the signal modeling step is a central and critical element that will determine the final accuracy of the surface moisture estimates. Different backscattering models can then be used to reproduce SAR signals in the bare soil period ([8–10]), while the vegetation component is estimated through the Water Cloud Model [11]. However, the soil model's performance is limited, even after modifications by calibration or taking into account the observed biases [12]. An alternative relies on the use of a statistical approach, offering higher performance regarding the estimation backscatter coefficients [13], provided that there are sufficient ground measurements during satellite acquisitions (so that calibration and validation steps can be carried out independently).

Regardless of the considered approach, the estimates are derived at spatial scales ranging from the regional (i.e., pixel of several km²) to the plot scale (i.e., area of interest of several hectares), while the possibilities of mapping at the intra-plot spatial scale are rarely addressed [1,4–7]. However, this spatial scale is a determining factor in the modulation of agricultural practices, particularly in the context of precision farming. It is, therefore, necessary to estimate the potential of SAR data for monitoring sub-surface parameters at spatial scales close to the pixel. Especially in a context where access to SAR images at metric or decametric spatial resolutions is made possible by several satellite missions (e.g., Sentinel-1, Radarsat constellation, Terrasar-X, and Tandem-X).

The objective of this study is to address the potential of TerraSAR-X data to estimate the surface soil moisture at the intra-plot spatial scale. The mean features of the quasi-synchronously collected ground data and SAR satellite images are described in Section 2. The proposed approach is based on a statistical algorithm (i.e., random forest), trained and validated by considering variable areas of interest (i.e., plot and intra-plot spatial scales). The results are analyzed and discussed (Section 3), focusing on the overall statistical performances obtained for images acquired at low and high incidence angles.

2. Experiments

2.1. Study Site

The network of plots was conducted where the experiment was located, in Southwestern France (Figure 1). From February to November 2010, in situ measurements of key sub-surface descriptors were regularly collected, synchronously with satellite images (MCM'10 campaign; see [14] for more details). The main characteristics of the study area were as follows: (i) a temperate climate, with an amplitude of mean monthly temperature near 20 °C (observed between winter and summer), and annual cumulative rainfall exceeding 600 mm; (ii) a highly anthropized area, with surfaces mainly allocated to seasonal crops cultivated on more than half of the landscape; (iii) a very fragmented landscape, with plots showing different shapes and sizes (with areas comprising between 1 and 95 hectares). In the present study, the focus was on bare soil conditions, which were observed after the harvest and before the sowing of the next crop (i.e., in spring and autumn).

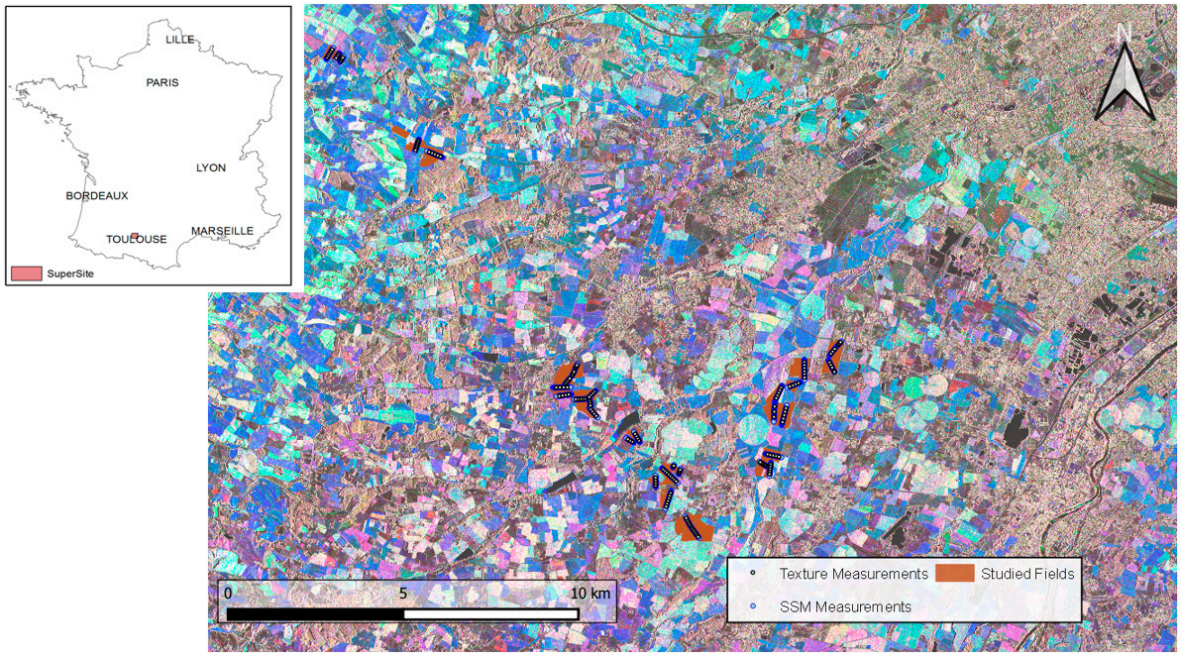

Figure 1. Location of the study site (super site) in Southwestern France. The network of the surveyed fields (brown polygons) superimposed on a color-composed TerraSAR-X image acquired in StripMap mode at HH polarization (red: 2010/05/20; green: 2010/08/16; blue: 2010/11/23). Soil moisture and texture measurements are represented by blue and black circles, respectively.

2.2. Materials

2.2.1. In Situ Data

The three key variables having a marked influence on the dynamics of the SAR signals in bare soil periods, and allowing to characterize the surface horizon, were collected on each monitored plot. The surface roughness was measured after each tillage event, using a 2 m-long needle profilmeter (composed of 201 needles spaced one centimeter apart). Two quantitative variables were derived from the couples of profiles recorded parallel and perpendicular to the direction of the tillage of the plot. The values of root mean square height (hrms) and the correlation length (lc) showed large variation intervals (varying from 0.5 to 6.9 cm, and 1.1 to 16.5 cm, respectively), consistent with the observed surface conditions (with smooth to very rough surfaces). Surface soil moisture (i.e., top soil layer of 0–5 cm) and texture geo-located measurements were performed along the same transects for each field. The fractions of clay, silt, and sand were derived from 2 to 8 points performed on each plot, consisting of 16 core samples within a circle of 15 m of diameter and a depth of 25 cm. A total of 146 points were collected, showing the dominance of the silt fraction within the study area (52% of silt and 24% of clay and sand, for average values) and an important variation of texture conditions with fractions between 22 and 77% for the silt, between 9 and 58% for the clay, and between 4 and 53% for the sand. The monitoring of SSM was performed using portable probes (ML2x from ThetaProbe), delivering a signal in mV, which was converted into volumetric moisture (using the calibration relationship established by [14]). The regular measurements of SSM were collected quasi-synchronously with satellite acquisitions (time lag between in situ measurements and satellite acquisitions of less than one day for the majority of cases), allowing us to characterize the soil under a wide range of moisture conditions (from dry to saturated), characterized by values of SSM ranging from 3.2 to 34.9%.

2.2.2. TerraSAR-X Satellite Data

The German satellite TerraSAR-X operating in the X-band (f = 9.65 GHz, λ = 3.1 cm) provided the 21 microwave images (Table 1). They were acquired at low (27.3°) or high

(53.3°) incidence angles (11 and 10 images, respectively) in HH polarization. Two beam modes (SpotLight and StripMap) characterized by a pixel spacing ranging from 1.5 to 2.75 m [15] were used. All images were calibrated; the backscattering coefficients were finally averaged at the plot scale considering six buffers with a radius ranging from 5 to 30 m (corresponding to areas from ~80 to ~2800 m²).

Table 1. Mean features of the TerraSAR-X images acquired with SpotLight (SL) and StripMap (SM) modes.

Mode	Acquisition Date	Orbit Pass	Incidence Angle (°)	Pixel size (m)
Spotlight	03/05/10; 05/21/10; 07/15/10; 08/17/10; 09/30/10 10/11/10; 10/22/10; 11/02/10; 11/13/10; 11/24/10	D	53.3	1.5
StripMap	02/21/10; 03/26/10; 05/09/10; 05/20/10; 07/14/10 08/16/10; 09/29/10; 10/10/10; 10/21/10; 11/12/10; 11/23/10	D	27.3	2.75

2.3. Method

The statistical algorithm proposed by [16] was used to estimate SSM, by considering the following inputs as explanatory variables: the backscattering coefficients and the incidence angles of the SAR images, the fractions of clay and sand, and the soil root mean square height (hrms) and correlation length (lc) collected in the parallel and perpendicular directions. The random forest method has been widely used in different fields, being particularly appropriate in the multi-factorial context to model non-linear relationships. The targeted variable is derived from a weighted mean of an ensemble of estimations, obtained from independent decision trees trained on different sets of samples. Such a procedure limits the problems of over-adjustment or the noise influence on data, and provides a high stability of results.

In the present study, independent cases were considered accordingly to the considered spatial scale, which was plot or intra-plot. Six buffer areas were taken into account by considering the geo-location of texture measurements as a reference and a radius ranging from 5 to 30 m (corresponding to areas from ~80 to ~2800 m²). These areas of interest were used to extract the SAR satellite signals and to select the corresponding SSM measurements.

Regardless of the considered spatial scale, the dataset was randomly partitioned into two subsets. The statistical algorithm was calibrated on the training set and validated on the independent test set. This procedure was repeated ten times. Finally, the average values of the coefficient of determination (R^2) and the root mean square error (RMSE) were derived from the comparison between the observed and estimated values of the SSM.

3. Results and Discussion

3.1. Overall Performances Obtained at the Plot Spatial Scale

The estimated values of SSM were compared to in situ measurements showing the independent subsets of samples used during the training and validation steps (in grey and black, respectively) (Figure 2). The levels of performance were close, regardless the considered incidence angle, with an RMSE of 5.12 and 4.96% $m^3.m^{-3}$, and R^2 of 0.64 and 0.66 (values obtained for the validation subset of samples). A quasi-similar magnitude of values was observed during the training step, pointing out the high stability of the results when using the RF algorithm. The level of accuracy, and in particular the correlation values, may appear to be limited; however, these results are consistent with a number of past studies performed in bare soils, using X-band SAR signal and empirical or semi-empirical models [1,4,5,7]. Although these approaches are different from the one implemented here,

the performance levels are equivalent to those obtained with the statistical approach, the best results showing SSM estimates with an R^2 ranging from 0.64 to 0.79 and an RMSE when presented varying between 2.81 and 4.09 $m^3.m^{-3}$. Moreover, in our case, the approach was applied over a wider soil roughness domain (hrms of 3.9 cm in the previous case compared to 6.9 cm in the present case), and independently to images acquired at two contrasting incidence angles (i.e., at 27.3 and 53.3°), without observing any noticeable difference in the level of performance. The absence of an angular effect constitutes an advantage of the proposed method, offering interesting prospects for estimating SSM using satellite images with various configurations.

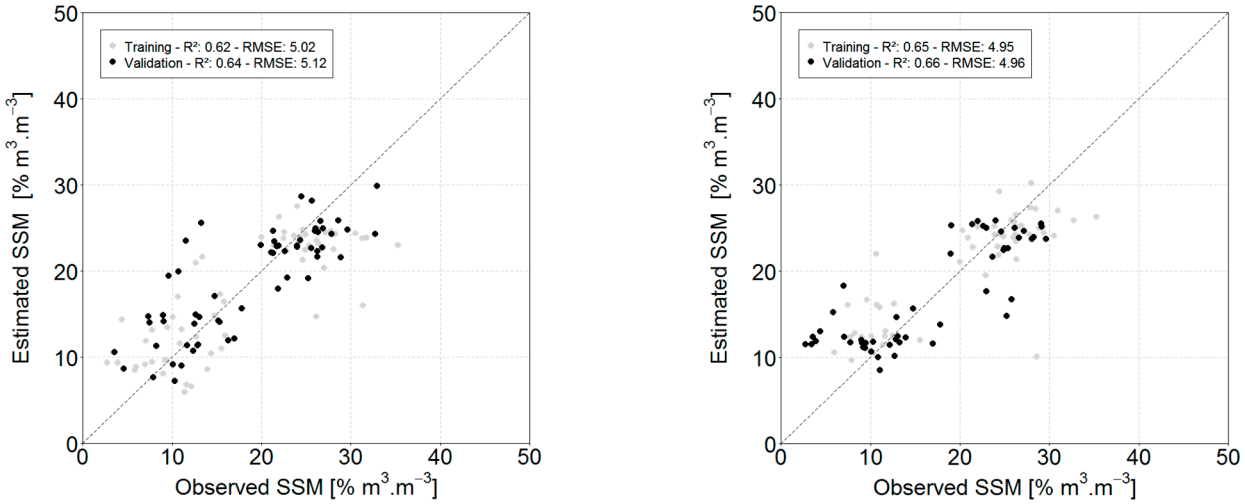

Figure 2. Comparison between in situ measurements of surface soil moisture and estimates derived from TerraSAR-X images acquired at 27.3° (**a**) or 53.3° (**b**). The grey and black dots represent the estimations performed considering the training or validation subsets of samples, respectively.

3.2. Evolution of the Statistical Performance at the Intra-Plot Spatial Scale

Figure 3 presents the statistical performances (R^2 and RMSE) obtained by comparing the values of SSM estimated using the statistical approach to ground measurements for circular buffers ranging from 5 to 30 m, together with results obtained at the plot scale. The performance increased in correlation from 0.46 to 0.78, while the error decreased from 6.45 to 3.97% $m^3.m^{-3}$, when considering the 5 and 30 m buffers. This gain in performance had a non-linear behavior and became weak when the radius of the buffer reached 20 m. This phenomenon is mainly explained by the specificities of the SAR signal, and in particular by the radiometric resolution. In a previous study, the authors of [17] characterize the radiometric resolution for the two TerraSAR-X beam modes used in the present study. For the considered intra-plot spatial scales, the values of radiometric resolution shift from 0.71 to 0.13 dB and from 1.14 to 0.21 dB, for the SL and SM beam modes, respectively. The non-linear performance gain observed with the increase in buffer size appears to be consistent with the exponential decrease in radiometric resolution values. Statistical performance is thus very close for buffers greater than a 20 m radius (radiometric resolution values being almost similar). Moreover, weaker performances obtained at the plot scale highlight the fact that SSM measurements performed locally do not significantly represent the surface state at the plot scale.

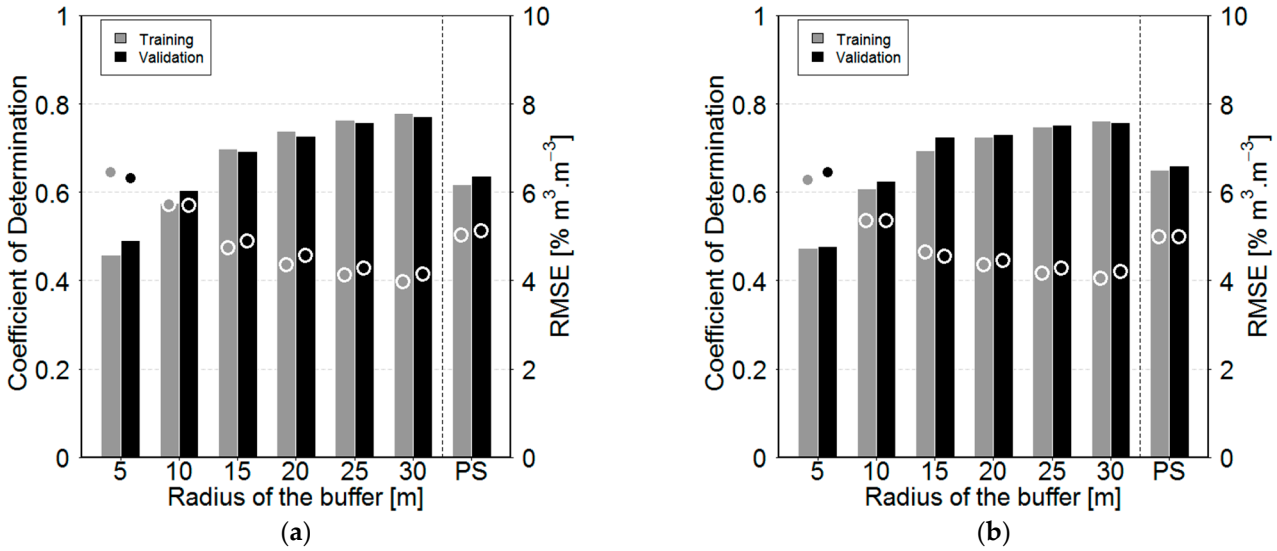

Figure 3. Evolution of the statistical performances (coefficients of determination and root mean square errors, bars and dots, respectively) with the buffer's size and at the plot spatial scale (PS), for the training (grey) or validation (black) subsets of samples and for SSM estimates derived from TS-X images acquired at low (27.3°) and high (53.3°) incidence angles (**a** and **b**, respectively).

Figure 4 presents a comparison between the estimated and in situ measurements of SSM values for the buffer of 30 m. At this spatial scale, a high level of performance was observed in both training and validation steps, regardless of the considered incidence angle. The values of R^2 exceeded 0.75, while the RMSE on SSM estimates was lower than 4.2% $m^3.m^{-3}$. SSM estimates, however, were associated with wide dispersion, although performance levels obtained at this spatial scale exceeded previous results obtained at the spatial scale of the plot [1,4,5,7].

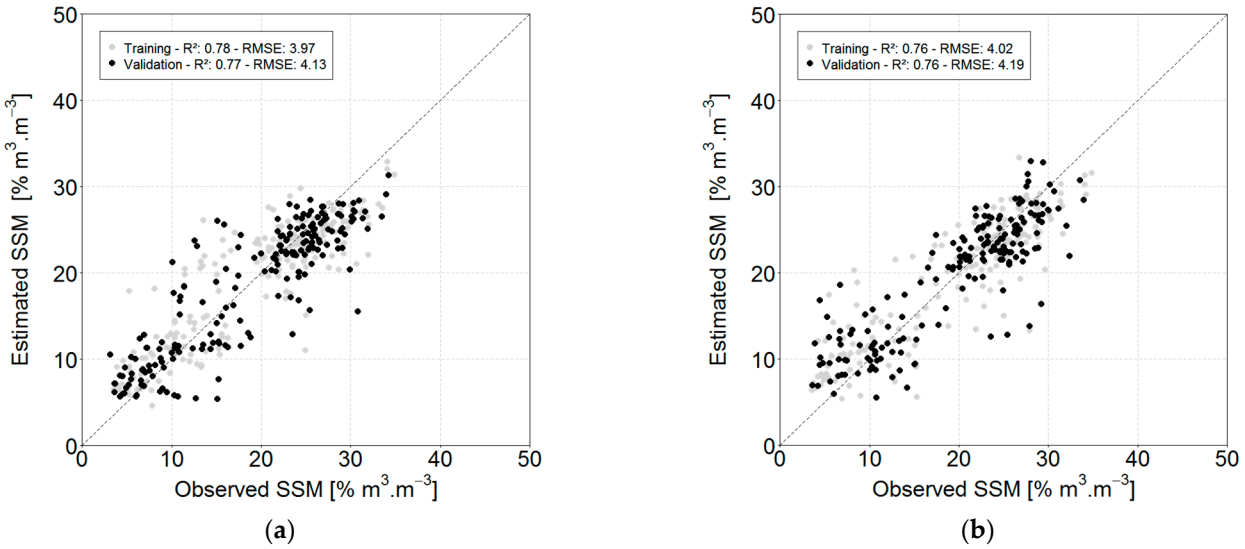

Figure 4. Comparison between estimated and observed SSM for a buffer with a radius of 30 m and for TS-X images acquired at low (27.3°) and high (53.3°) incidence angles (**a** and **b**, respectively). The grey or black colors represent the estimations performed considering the training or validation subsets of samples, respectively.

5. Conclusions

The present study took advantage of a dense network of georeferenced in situ measurements collected synchronously with the regular acquisition of X-band SAR images to address the potential of high-spatial resolution TerraSAR-X data for surface soil moisture

estimation at the intra-plot scale. Results based on a statistical algorithm were obtained from images with low and high incidence angles (i.e., 27.3 and 53.3°), showing performance levels consistent with the literature at the plot scale and particularly promising results at the intra-plot scale (R^2 superior to 0.75 and RMSE lower than 4.20 $m^{-3}.m^{-3}$ over areas of 2800 m^2, regardless of the incidence angle).

The actual or planed satellite missions offer a wide range of possibilities that should be tested with the method presented here, by considering images acquired at different frequencies, at contrasting angles of incidence, or with different polarization states. The only constraint lies in the availability of data, especially in situ, in order to be able to implement the statistical approach. Moreover, the characteristics of the satellite sensors, as well as the beam modes of image acquisition, condition the SAR signal that needs to be tested to determine the possibilities for intra-plot scale studies offered by other satellite missions.

Author Contributions: The authors contributed equally to the various steps required to complete this study. All authors have read and agreed to the published version of the manuscript.

Institutional Review Board Statement: Not applicable.

Informed Consent Statement: Not applicable.

Data Availability Statement: The data presented in this study are available on request from the corresponding author.

Acknowledgments: Authors would like to thank Space Agencies for their support and confidence in this project (CNES, ESA, and DLR). Many thanks go to the farmers and people who helped in collecting ground data.

Conflicts of Interest: The authors declare no conflict of interest.

References

1. Baghdadi, N.; Aubert, M.; Zribi, M. Use of TerraSAR-X data to retrieve soil moisture over bare soil agricultural fields. *IEEE Trans. Geosci. Remote Sens. Lett.* **2012**, *9*, 512–516.
2. Maleki, M.; Amini, J.; Notarnicola, C. Soil roughness retrieval from TerraSar-X data using neural network and fractal method. *Adv. Space Res.* **2019**, *64*, 1117–1129.
3. Zribi, M.; Kotti, F.; Lili-Chabaane, Z.; Baghdadi, N.; Ben Issa, N.; Amri, R.; Amri, B.; Chehbouni, A. Soil texture estimation over a semiarid area using TerraSAR-X radar data. *IEEE Trans. Geosci. Remote Sens. Lett.* **2012**, *9*, 353–357.
4. Aubert, M.; Baghdadi, N.; Zribi, M.; Douaoui, A.; Loumagne, C.; Baup, F.; El Hajj, M.; Garrigues, S. Analysis of TerraSAR-X data sensitivity to bare soil moisture, roughness, composition and soil crust. *Remote Sens. Environ.* **2011**, *115*, 1801–1810.
5. Gorrab, A.; Zribi, M.; Baghdadi, N.; Mougenot, B.; Chabaane, Z.L. Potential of X-Band TerraSAR-X and COSMO-SkyMed SAR data for the assessment of physical soil parameters. *Remote Sens.* **2015**, *7*, 747–766.
6. Mirsoleimani, H.R.; Sahebi, M.R.; Baghdadi, N.; El Hajj, M. Bare soil surface moisture retrieval from Sentinel-1 SAR data based on the calibrated IEM and Dubois models using neural networks. *Sensors* **2019**, *19*, 3209.
7. El Hajj, M.; Baghdadi, N.; Zribi, M.; Belaud, G.; Cheviron, B.; Courault, D.; Charron, F. Soil moisture retrieval over irrigated grassland using X-band SAR data. *Remote Sens. Environ.* **2016**, *176*, 202–218.
8. Oh, Y.; Sarabandi, K.; Ulaby, F.T. An empirical model and an inversion technique for radar scattering from bare soil surfaces. *IEEE Trans. Geosci. Remote Sens.* **1992**, *30*, 370–381.
9. Dubois, P.C.; van Zyl, J.; Engman, T. Measuring soil moisture with imaging radars. *IEEE Trans. Geosci. Remote Sens.* **1995**, *33*, 915–926.
10. Fung, A.K.; Li, Z.; Chen, K.-S. Backscattering from a randomly rough dielectric surface. *IEEE Trans. Geosci. Remote Sens.* **1992**, *30*, 356–369.
11. Attema, E.P.W.; Ulaby, F.T. Vegetation modeled as a water cloud. *Radio Sci.* **1978**, *13*, 357–364.
12. Fieuzal, R.; Baup, F. Improvement of bare soil semiempirical radar backscattering models (Oh and Dubois) with SAR multispectral satellite data (at X, C and L bands). *Adv. Remote Sens.* **2016**, *5*, 296–314.
13. Fieuzal, R.; Baup, F. Statistical estimation of backscattering coefficients in X-band over bare agricultural aoils. In Proceedings of the 2020 Mediterranean and Middle-East Geoscience and Remote Sensing Symposium (M2GARSS), Tunis, Tunisia, 9–11 March 2020; pp. 302–305.

14. Baup, F.; Fieuzal, R.; Marais-Sicre, C.; Dejoux, J.-F.; le Dantec, V.; Mordelet, P.; Claverie, M.; Hagolle, O.; Lopes, A.; Keravec, P.; et al. MCM'10: An experiment for satellite multi-sensors crop monitoring from high to low resolution observations. In Proceedings of the 2012 IEEE International Geoscience and Remote Sensing Symposium, Munich, Germany, 22–27 July 2012; pp. 4849–4852.
15. Breit, H.; Fritz, T.; Balss, U.; Lachaise, M.; Niedermeier, A.; Vonavka, M. TerraSAR-X SAR processing and products. *IEEE Trans. Geosci. Remote Sens.* **2010**, *48*, 27–40.
16. Breiman, L. Random Forests. *Mach. Learn.* **2001**, *45*, 5–32.
17. Fieuzal, R.; Marais, S.C.; Baup, F. Estimation of corn yield using multi-temporal optical and radar satellite data and artificial neural networks. *Int. J. Appl. Earth Obs. Geoinf.* **2017**, *57*, 14–23.